Journal of the American Helicopter Society, Volume 64, Issue 3, 2019, pp. 1-14
DOI: 10.4050/JAHS.64.032004

The Effect of Steady and Pulsed Air Jet Vortex Generator Blowing on a Aerofoil Section Model Undergoing Sinusoidal Pitching

Simon Prince

School of Aerospace, Transport & Manufacturing, Cranfield University, UK

Richard Green & Frank Coton

School of Engineering, University of Glasgow, UK

Yaxing Wang

School of Engineering, University of Liverpool, UK

Abstract

Experimental results are reported on the assessment of steady and pulsed air jet vortex generators (AJVGs) for the suppression of dynamic stall on a sinusoidal pitching RAE9645 aerofoil model. Tests at Re_c of 1 million, at reduced pitching frequencies between 0.01 and 0.10 were performed with and without steady and pulsed AJVG blowing. The effect of jet momentum coefficient ($0.0003 < C_\mu < 0.0046$), jet duty cycle ($0.25 < DC < 1$) and jet pulsing frequency ($0.29 < F^+ < 2.93$) were investigated. Pulsed air jet blowing with F^+ in the range 0.5 – 1.0 and with a duty cycle in the range 0.4 – 0.5, was found to be the most effective to achieve full suppression of dynamic stall vortex formation.

Footnote text should indicate if paper was presented at National Meeting or other conference.

Nomenclature

a = damping coefficient (computed with angles in radians)

b = model span, *m*

c = chord length, *m*

C_N = normal force coefficient based on model planform area

C_M = quarter chord pitching moment coefficient based on model planform area

C_p = pressure coefficient

C_μ = jet momentum coefficient, $\dot{m}U_j / q_\infty cb$

C_w = work coefficient (computed with angles in radians)

d = jet orifice diameter, *mm*

δ = local boundary layer height, *mm*

DC = jet duty cycle (from 0 to 1)

f = jet blowing frequency, *Hz*

F^+ = nondimensional jet blowing frequency; $f x_{TE} / U_\infty$

k = nondimensional aerofoil pitching frequency, $\omega \mathbf{c} / 2U_\infty$

$\dot{m}$ = jet mass flow rate, *kg/s*

p = air jet vortex generator plenum pressure, *Pa*

p_∞ = wind tunnel freestream pressure, *Pa*

q_∞ = freestream dynamic pressure, *Pa*

Re_c = Reynolds number based on chord

U_∞ = wind tunnel freestream speed, *m/s*

U_j = jet velocity, *m/s*

VR = jet to freestream velocity ratio

x = chordwise distance, *m*

x_{TE} = chordwise distance from the jet orifice to the trailing edge, *m*

y = distance normal to the aerofoil chord, *m*

α = aerofoil angle of attack, *deg*

$\bar{\alpha}$ = mean (collective) aerofoil angle of attack during sinusoidal pitch motion, *deg*

$\hat{\alpha}$ = cyclic (half amplitude) aerofoil angle of attack, *deg*

ω = aerofoil sinusoidal pitching frequency, *rad/s*

1. Introduction

The phenomenon of dynamic stall considerably restricts the safe flight envelope of conventional helicopters. On the retreating blades of the main rotor cyclic pitch imposes a relatively large angle of attack. Here, when the blade is also experiencing its lowest oncoming flow speed, the rotor blade will undergo low speed separation which often results in dynamic stall. This is the extremely rapid process by which the separation front jumps forward, usually when the rotor is experiencing its rapid pitch down motion, all the way to the leading edge causing the formation of a very strong stall vortex. While this vortex is rapidly shed, the suction from its strong core momentarily causes very high lift and drag forces and pitching moments, which are detrimental to the aircraft performance and fatigue life of the rotor system. The process is described in detail in references 1and 2.

This paper presents the findings of an experimental study to assess how blowing using air jets may be used to control dynamic stall in low speed incompressible flow conditions. In particular the aim is to investigate the effect of pulsed and steady air jet vortex generators and to characterise the effect of blowing momentum, duty cycle and pulsing frequency at different aerofoil pitching rates. The results are publicly available, (https://doi.org/10.17862/cranfield.rd.5001947), for the computational simulation community for the purposes of code validation for this highly challenging unsteady flow phenomena.

2. Dynamic Stall Suppression Using Air Jet Blowing

The application of jets of air, blown into a boundary layer to promote turbulent mixing and re-energisation to suppress flow separation and subsequent stall, was first reported by

Wallis (Ref. 3) in 1952. Since then many studies have been performed and different steady and periodic blowing actuation concepts developed. Air jet vortex generators (AJVGs) involve blowing a directed jet through a narrow orifice skewed at an angle to the oncoming flow and set to a pitch angle relative to the local surface tangent.

A number of studies (Refs. 4 – 10) reported that the maximum vorticity, and thereby mixing intensity, generated within a boundary layer is achieved with an air jet skew angle in the range 45^o – 60^o to the oncoming flow, and with a pitch angle of between 30^o and 45^o. AJVGs act in exactly the same way as the more conventional vane vortex generator, promoting mixing by the development of boundary layer embedded streamwise vortices that entrain high energy air from the outer regions of the boundary layer and sweep it down into the lower layers. They have been shown to achieve a delay in static stall angle similar to those achieved using vane vortex generators, but with the advantage that they do not impose a permanent and significant excrescence drag as they can be deactivated when not needed.

In the early 1970s, Oyler and Palmer (Ref. 11) undertook one of the first studies of the effect of periodic blowing into a boundary layer. They investigated the effect of unsteady tangential blowing on a trailing edge flap and demonstrated a significant improvement in stall suppression and maximum lift capability over and above that delivered with steady blowing with the equivalent mass flow. Since then many investigators have confirmed that oscillatory or pulsed blowing for the suppression of boundary layer separation is more effective than steady blowing, with the added benefit of reduced mass flow requirements (Refs. 12 – 28).

Seifert et al. (Ref. 12) applied unsteady blowing, through slots, to a NACA 0012 wing section with trailing edge flap. The experiments, performed at Reynolds number based on chord of between 10^5 and 10^6, measured the aerodynamic characteristics under quasi-steady pitch conditions. Unsteady blowing was shown to achieve equivalent stall suppression capability as steady blowing but for an order of magnitude less total mass flow and power consumption. McManus et al. (Refs. 13 & 14) demonstrated the ability of unsteady, oscillatory blowing, AJVGs to supress the separation of a turbulent boundary layer from a 20° ramp diffuser section. In this case the Reynolds number was relatively low, being 2300 based on the local undisturbed boundary layer thickness, δ, at the plane of the jet orifices, some 8δ upstream of the ramp edge. Pulsed laser sheet illumination with acetone vapour seeding revealed that each air jet pulse created a large-scale coherent vortical structure embedded in the boundary layer. These features convected downstream within the boundary layer enhancing the mixing in a manner completely different to that, involving strong continuous streamwise vortices, with steady AJVG blowing. It was also shown that, for a given total mass flow rate, oscillatory AJVGs are more effective in suppressing turbulent boundary layer separation than equivalent steady blowing.

A further study investigating unsteady slot blowing by Seifert et al. (Ref. 15) involved the periodic blowing from the upper surface of a trailing edge flap mounted on the rear of four different aerofoil main elements. This set of experiments, performed at Re_c in the range $0.15 – 1.2\text{x}10^6$, revealed the importance of the frequency of jet pulsing. The results showed that the most effective reduced pulsing frequency, F^+, was around 1.0.

McManus et al. (Refs. 16 & 17) demonstrated the importance of the jet to freestream velocity ratio, VR, in experiments to suppress stall using pulsed AJVGs on a stylized

aerofoil section. The model comprised two flat plate sections, the leading edge section having a length of ~21% of the model chord and being deflected down relative to the rear section by 15°. The single circular orifice air jet was located close to the corner edge and was pitched and skewed at 45° and 90° to the freestream flow direction respectively. Tests were performed at a constant Re_c of 0.5×10^6, with the air jet pulsed in the frequency range 10 – 100 Hz and at jet to freestream velocity ratios in the range 1.5 – 6.0. The results demonstrated that pulsed AJVG blowing suppressed stall from 12° angle of attack to 16°, while increasing *VR* and mass flow rate improved AJVG performance. A parametric study showed that the optimum pulsing frequency was dependent upon the value of *VR*. For $VR \leq 2$, it was found that optimum $F^+ \approx 0.5$, while for $VR > 2$ optimum F^+ reduced to around 0.4. A link was also suggested between the optimum pulsing frequency and the natural shedding frequency of the eddies in the separated flow.

The importance of jet *VR* was further demonstrated in the experiments of McManus and Magill (Refs. 18 & 19) involving the control of the flow around a NACA 4412 main section aerofoil with a leading edge slat of chord 20% of the overall model chord. For Mach numbers between 0.1 and 0.5 the tests demonstrated improved performance with increasing VR, while an optimum reduced pulsing frequency of $F^+ \approx 0.6$ was found. The difference in optimum F^+ between this study and McManus et al.'s earlier results suggest that the effect of pulsing frequency is sensitive to geometry or pressure gradient. Greenblatt et al. (Refs. 20, 24 & 25) undertook a number of experimental studies into the effect of pulsed blowing. These studies showed that the most effective location for a pulsed air jet array is in the vicinity of the separation front, and that optimum F^+ was in the range 0.5 – 1.0. Scholz et al. (Ref. 21) investigated the capability of an array of pulsed air jets located near the leading

edge of an aerofoil model to suppress abrupt leading edge separation. These experiments were performed at Re_c of 1.3×10^6, with an array of 80 rectangular air jet orifices skewed at 45^o to the freestream flow. It was found that the array of jets, located on the upper surface only 1% of chord from the leading edge, could not prevent separation but were found to increase normal force coefficient above the prestall value. Pulsing frequency was not found to have a significant effect in this case but the aerodynamic characteristics were found to be sensitive to jet duty cycle, the best results being obtain with duty cycle in the range 0.12 – 0.25.

Ortmanns et al. (Ref. 22) used phase locked stereoscopic PIV to track the coherent turbulent structures generated within a turbulent boundary layer on a flat plate model in a water tunnel. In this study the jet *VR* and pulsing duty cycle was varied with a fixed pulsing frequency of 1Hz. A velocity overshoot was seen to occur at the beginning of each pulse with the result that enhanced mixing was observed with larger and stronger vortical structures. This start-up effect, which was sensitive to *VR* but not to duty cycle, was found to be an important factor in the study of Prince et al. (Ref. 28) who implemented a velocity overshoot in the air jet velocity profile in their study of the effect of pulsing AJVGs for low speed stall suppression. In this study a RAE 9645 aerofoil section model was fitted with an array of pulsed air injectors that could be operated in steady blowing mode or at pulsing frequencies up to 300Hz. A parametric study of the effect of air jet to freestream velocity ratio, pulsing duty cycle and reduced pulsing frequency was performed with Re_c of 1.1×10^6. This study also demonstrated the significantly improved effectiveness of pulsing AJVGs over steady blowing ones in the suppression of trailing edge separation and subsequent stall. A correlation was found between the measured aerofoil trailing-edge

shedding frequency and the maximum normal force enhancement. The maximum normal force coefficient was achieved at a reduced pulsing frequency of $F^{+}\approx 0.6$, corresponding with the natural shedding frequency of the stalled aerofoil. Surface tuft visualisation was used to reveal what looked like periodic wavelike motions of the separation front downstream of the air jet orifices for the case of low frequency pulsing. This suggested that the advance and retreat of the separation front was synchronised with the pulsing of the air jets.

For the case of AJVGs applied to aerofoils in pitching motion, a much more limited body of data is available. Greenblatt et al. (Refs. 24 & 25) showed that in order to ensure a train of many coherent vortical structures exist at any moment during the pitch up motion, much higher frequencies (typically higher than 200Hz) are necessary for dynamic stall suppression than for static stall suppression. A threshold value of VR was found beyond which increases did not result in further improvements in lift enhancement. In this case this was found to be around $VR \approx 4$. In addition, the duty cycle was not found to be as sensitive in these series of experiments under dynamic pitching conditions. Weaver et al. (Ref. 26) undertook tests of tangential blowing from the quarter chord location on a Boeing Vertol *VR-7* aerofoil during sinusoidal pitching conditions in a water tunnel at Re_c of $1\text{x}10^5$. With blowing rates between $C_\mu = 0.16$ and 0.66, steady blowing at the higher blowing rate was sometimes found to suppress the bursting of the leading edge separation bubble responsible for stall vortex formation. In general the steady blowing was found to reduce the load hysteresis characteristics. Pulsed blowing was also investigated where the optimum reduced pulsing frequency was found to be $F^{+}\approx 0.9$. Gardner et al. (Ref. 27) compared pulsed air jet blowing with steady blowing on an OA209 aerofoil, where an array of 42

orifices at 10% chord location on the upper surface was employed, each of 1% chord diameter. They found that at Mach 0.3, and Reynolds number 530,000 light stall could be almost completely suppressed with constant blowing at C_μ =0.08. In deep stall conditions steady blowing was found to be able to reduce peak pitching moment by 65%. Pulsed blowing at high frequencies (between 100 – 500 Hz) with the same mass flux was found to be as effective at suppressing dynamic stall as constant blowing. Müller-Vahl et al. (Ref. 28) developed what they called "adaptive blowing", which involved the active sensing and optimisation of the unsteady blowing profile to best minimize lift force excursions. This was applied to a NACA 0018 model and tested at Re_c in the range 1.5 – 5.0x10^5. Blowing was applied to the upper surface near the leading edge and was tested with the model undergoing pitch oscillations as well as with fixed pitch with rapid freestream oscillations. The investigators were successful in fully suppressing dynamic stall and in achieving almost constant phase averaged lift.

3. Experimental Details

The test model developed for the experiments used the RAE9645 aerofoil profile, representative of a modern helicopter rotor section, and was constructed with a chord length of 0.5m. The effective span of the model, between the end plates, was 1.1m. Oval end plates were fitted to maintain quasi-2D spanwise flow behaviour. The model was constructed out of moulded fibre glass upper and lower surface sections with internal insert sections to provide support. The internal pressure regulated plenum chamber used to feed the air jets was constructed from a high pressure plastic pipe, installed inside the model with the air being fed in at the same pressure at both ends. The air jet orifices, located in

an array of 20 at 12% chord on the upper surface, were set with a spacing, between each one, of 45mm. Each orifice had a circular cross-sectional area of 18mm^2. They were pitched at 30^o from the surface tangent and skewed at 60^o with respect to the free-stream direction, to match the experimental arrangement of reference 28,. The pitch and skew angles used at the jet exits were arranged to induce co-rotating streamwise vortices over the aerofoil upper surface for the steady blowing cases, the settings being those which the literature suggests are optimum for the generation of maximum vorticity in the downstream boundary layer. The geometrical orientation, shape and individual spacing of the AJVGs installed on the model were based on design guidelines outlined by previous researchers (Refs. 9 -14).

The internal AJVG actuator / ducting system consisted of the plenum pipe which fed all of the 20 jets and was pressure regulated, small tubes which connected it to the pulsed air injectors and a specially designed jet nozzle module, as shown in figure 2a) with a short, constant circular cross sectional area, duct delivering the air jet to the surface. The air jet nozzle modules were designed as a plastic insert to link the air injectors with the upper surface orifices in such a way as to ensure the correct orifice pitch and skew angle while maintaining a smooth and continuous upper surface profile.

The Synerject pulsed air injector, shown in figure 2b), is based on IC engine solenoid fuel injector technology and was chosen as the pulsed air jet actuator since it was found to satisfy the required mass flow, pulsing characteristics and geometrical size requirements. The air jet / injector / plenum assembly was isolated from the model structure, as much as possible, with vibration dampening material in an effort to reduce the vibrational noise

emitted from the injectors affecting the pressure sensors. Figure 3 presents a typical air jet exit pressure trace, for a square wave input signal.

The model was instrumented with a total of 39 dynamic pressure transducers, flush mounted in surface pressure tappings, positioned at centre-span along the chordline. These transducers were rated at 34kPa range, and their chordwise locations are plotted in figure 1, along with the location of the AJVG array. An additional 10 dynamic pressure transducers were mounted on the upper surface a spanwise distance 8.5mm to one side of the main transducer array. These were used primarily as a mean to verify the measurements on the main transducer array. The resulting pressure distributions were then integrated to calculate the aerodynamic forces and moments, neglecting the effects of surface skin friction. The plenum chamber pressure was measured by use of a differential pressure transducer mounted centrally inside the pipe wall.

Output signals from these transducers were processed by a specially designed signal-conditioning unit with an internal control board. The control board automatically removed all offsets and adjusted the gains as necessary. This was done, during a typical test, by computer sampling the maximum and minimum of each transducer output and adjusting the gains to improve the data acquisition resolution. The data acquisition was carried out by a PC interfaced with proprietary Bakker Electronics BE256 modules that provided the analogue to digital conversion. The TEAM 256 software was used for data acquisition.

The measurement system had a capability of measuring up to 200 channels, with each Analogue-Digital channel having a maximum sampling rate of 50kHz. Such a high sampling rate was required to capture the fine detail of the high speed dynamic stall process, especially at the highest oscillatory frequencies or pitch rates. The surface data for

the oscillatory pitching tests was acquired in four blocks of data, totalling 32000 samples. The sampling rate was set according to the pitching frequency, and the four blocks of data were averaged to give the final results. Data acquisition commenced after a minimum of five pitch cycles, with recording taking place over the next five cycles. The data were then phase averaged over these five cycles. Close scrutiny of the instantaneous data showed that cycle to cycle variation was minor, amounting to ΔC_p of no more than ±0.04.

The difference between the static pressure in the working section, 1.2m upstream of the leading edge, and the static pressure in the settling chamber was measured by a FURNESS FC012 micromanometer for the purposes of calibrating the working section and model measurement systems.

An angular displacement transducer geared to the shaft of the rotating model measured the instantaneous angle of attack of the aerofoil section model. The signal voltage from the transducer was fed into an amplifier/splitter to produce three signals for the following purposes:

- Connection to the multiplexer for the high speed recording of the aerofoil angle of attack,
- Connection to the Schmitt trigger for initiation of data sampling when a preset angle (voltage) was reached, and
- A feedback signal to the hydraulic actuator controller.

The experiments were performed in the Glasgow University Handley-Page low speed, closed circuit, wind tunnel. The RAE 9645 model was mounted vertically in the octagonal 2.13m x 1.61m working section, being pivoted about two tubular steel shafts connected, via two self-aligning bearings, to the support frame, as shown in figure 4. The steel shafts,

which act as the axis of pitch rotation of the model, were fixed through the model quarter chord axis. The weight of the model was carried through a thrust bearing on the upper support beam, while the aerodynamic loads were borne by both the upper and lower support beams, connected to the steel tunnel frame.

The oscillatory motion of the model was achieved using a UNIDYNE 907/1 hydraulic linear actuator mounted on the support frame underneath the working section and connected, via a crank mechanism, to the model mounting shafts. The UNIDYNE actuator, rated with a normal dynamic thrust of 6.1kN, was driven by a 7.0MPa supply pressure and controlled via a MOOG 76 series 450 servo-valve and UNIDYNE servo controller unit. Displacement measurement and feedback signal for the actuator controller was provided by a precision linear angular displacement transducer mounted on the lower support beam and geared to the model mounting shaft, as shown in figure 4, which provided instantaneous angle of attack to an accuracy of $\pm 0.1^{o}$.

The accuracy of the surface pressure measurements is estimated to be $\Delta C_p = \pm 0.02$ at the 30m/s freestream airspeed used in these tests. The integrated normal force and pitching moments are estimated to be within 5% of those measured by a force balance at zero angle of attack, improving to within 1% at high angle of attack, based on the findings from the analysis of a similar test (Ref. 23). Air jet momentum coefficient, C_μ, was determined by the measurement of the plenum pressure during the experiments, to obtain mass flow rate of the feed air, calibrated using an airflow meter. The jet velocity was obtained using a fine pitot probe which was traversed through the exit jet, normal to the jet axis, some 2mm from the jet orifice. The velocity was then averaged across the jet.

Pulsed jet momentum coefficient was estimated by factoring by the pulsed waveform duty cycle, so that the correct averaged mass flow is used. The accuracy of the C_μ measurements is estimated to be ±0.00001.

4. Results

4.1 The Effect of Steady and Pulsed Air Jet Blowing

The upper surface C_p variation with angle of attack for the RAE 9645 aerofoil section model undergoing oscillatory, 12.38rad/s (k = 0.103), 8 degree amplitude pitching was compared for the cases of 241kPa steady air jet blowing (C_μ =0.0026), 172kPa, 71Hz pulsed air jet blowing (C_μ =0.00075, F^+= 1.04, DC=0.5) and the clean aerofoil across the mean angle of attack range 6º to 20º. Figure 5 presents carpet plots of the upper surface C_p over one complete cycle for these conditions for the sample cases $\bar{\alpha}$=12º and 20º. Up to a mean angle of attack of 10º, there is negligible difference between the upper surface C_p carpets for the three cases. This is to be expected for the lowest mean angles of attack since, based on the quasi-static results, trailing edge separation occurs at α=11º and viscous effects only begin to take effect after about α=15-16º. At $\bar{\alpha}$=12º the first evidence of a dynamic stall vortex trace exists in the upper surface pressure carpet. This appears as a ripple like feature that begins as a weak disturbance near the leading edge at about α~20º (the beginning of the downstroke) and is shed from the trailing edge at α~15º. This ripple is in fact the suction trace of the dynamic stall vortex core on the upper surface, which is shed from the leading edge and very rapidly convects over the upper surface and past the

trailing edge, as described in previous work (Refs. 29 & 30). The formation, migration and shedding of the stall vortex is seen to occur on a very fast time scale, the event taking place within about 2° angle of attack at the start of the downstroke movement. At the oscillation frequency of 12.38rad/s (k = 0.103), this equates to an event that takes just less than 10ms. The feature is completely absent in the upper surface C_p carpet with steady 241kPa (C_μ =0.0026) air jet blowing, suggesting that for this oscillatory pitching condition, steady air jet blowing can be completely effective in suppressing the formation and shedding of a dynamic stall vortex. This agrees with previous findings (Refs. 29 & 30). The upper surface C_p carpet for the pulsed air jet blowing case appears to be almost identical to that for steady blowing, with no clear trace of dynamic stall vortex suction, except the appearance of some oscillations at the trailing edge. These small oscillations do not appear to resemble the ripple ridges that one would expect of a dynamic stall trace, and are much more likely to be due to model vibration and/or noise from the pulse jet actuators inside the model. It can therefore be concluded that for this oscillatory motion, pulsed air jets also appear to be effective in completely suppressing the formation and shedding of the dynamic stall vortex, with much less than half of the total air mass flow than that used for the steady air jet blowing.

For the $\bar{\alpha}$=14° case, a strong dynamic stall was seen with no air blowing, with a sharp leading edge suction peak followed by an abrupt drop in $-C_p$. A strong suction ridge was then visible stretching across the pressure plateau to the trailing edge. With 241kPa (C_μ =0.0026) steady blowing a weak trace of a stall vortex was visible together with a much weaker, and later collapse in, leading edge suction. The leading edge suction peak was seen to be much broader / less sharp, indicating a more benign dynamic stall event. The

corresponding suction trace is very weak, indicating that while steady blowing at 241kPa has not prevented the occurrence of dynamic stall, and the migration and shedding of a stall vortex, it has delayed the formation and reduced considerably the strength of the stall vortex. With 172kPa, 71Hz, (C_μ=0.00075, F^+= 1.04) pulsed air jet blowing the leading edge suction peak remained very rounded, as would be expected without any strong stall taking place. Small oscillations on the top of this suction peak would suggest an incipient stall event, and the small oscillations in the pressure plateau region towards the trailing edge are more extensive than for $\bar{\alpha}$=12° which might be evidence of an extremely weak stall vortex, but this is certainly not conclusive. What can be said with certainty is that the 172kPa pulsed air jet blowing has been more successful in suppressing dynamic stall for this case than 241kPa steady blowing.

For the more severe cases of $\bar{\alpha}$ =16° and above the C_p carpets followed similar trends and are represented in figure 5 by results for the extreme case of $\bar{\alpha}$ =20°. Now a strong dynamic stall vortex suction ridge is observed for all three cases. In fact there appears to be evidence of two suction ridges – a primary and a weaker secondary stall vortex. For the $\bar{\alpha}$=16° case steady blowing at 241kPa suppressed the secondary stall vortex suction ridge, and a secondary leading edge suction peak is observed that does not exist in the case of the clean aerofoil. This indicates that the steady blowing is acting to promote the reattachment of the upper surface boundary layer close to the leading edge, and thereby promote recovery of leading edge suction, in the post stall period during the downstroke. Pulsed, 172kPa air jet blowing at 71Hz pulsing frequency was also seen to suppress the formation of the secondary stall vortex suction ridge, indicating that this secondary vortex is not

generated in this case. Both modes of air jet blowing were still found to improve the overall aerodynamic performance at this more severe mean angle of attack.

For the next highest mean angle of attack of 18°, and for the highest 20° case, reproduced in figure 5, AJVG blowing, both 241kPa steady and 172kPa pulsed, did not appear to affect the upper surface C_p response carpets. For all three cases a very sharp full stall event takes place at around α=24°, with no post stall primary vortex recovery until nearly 10° angle of attack on the downstroke. For both cases, air jet blowing appeared to increase the peak leading edge suction from $C_p \approx$ -12 to -13. For these most severe, highest $\bar{\alpha}$ cases, the effects of air jet blowing appeared to be negligible.

In summary, the analysis of the upper surface C_p versus α carpets shows that AJVG blowing with C_μ =0.0026 at x/c~10% for M=0.1 and Re_c=1.0x10^6, can be effective in delaying the onset of dynamic stall, and improving the post stall aerodynamic characteristics for oscillatory pitching with moderate maximum angle of attack (α_{max} = 18-20°). In particular, C_μ =0.00075, F^+= 1.04 pulsed air jet blowing is seen to better suppress the secondary stall vortex formation. For very severe oscillatory pitching cases with maximum α above about 20°, the data suggests that air jet blowing (both steady and pulsed) has little effect in improving the aerodynamic characteristics.

Figure 6 presents the comparison of the results for the three cases - clean aerofoil, steady 241kPa (C_μ =0.0026) blowing and 172kPa pulsed (C_μ =0.00075, F^+= 1.04) blowing for C_N, and C_M respectively. The graphs are plotted for each mean angle of attack, the oscillation amplitude being constant at $\hat{\alpha}$ =±8°. The curves for C_N are plotted on the left of the figure. At the lowest mean angle of attack, $\bar{\alpha}$=6°, there is no evidence of any occurrence of stall or the subsequent hysteresis between the upstroke and downstroke normal force.

This is to be expected as the maximum angle of attack of 14° is below the α=15-16° at which the quasi-static pitching results indicate that the forward movement of the separation line from the trailing edge begins.

A very small degree (ΔC_N < 0.1) of hysteresis between the upstoke curve and the downstroke curves is seen for $\bar{\alpha}$=8° in the clean aerofoil case but this is suppressed completely by both steady 241kPa and pulsed 172kPa AJVG blowing. This corresponds with the results of the quasi-static pitching tests which repeatedly showed, for the same freestream conditions, that incipient trailing edge separation could be effectively delayed to α=13° by both steady and pulsed blowing at moderate blowing pressures, and that the onset of the effects of viscosity could be likewise delayed by about two degrees angle of attack. Increasing $\bar{\alpha}$ to 10° results in a more pronounced hysteresis loop in C_N curve, where the C_N level at a given angle of attack on the downstroke is less than the corresponding level on the upstroke, in the range 12° < α < 18°, with steady blowing. For the clean aerofoil case the hysteresis "loop" is seen to be considerably larger, and extends on the downstroke all the way to a recovery at α=10°. With pulsed 172kPa AJVG blowing, the hysteresis loop is smaller than that seen with 241kPa steady blowing, indicating improved suppression of the forward movement of the upper surface separation line which was also seen under quasi-static pitching (Ref. 23).

With $\bar{\alpha}$=12° the downstroke recovery occurs at α=7° for the unblown model, but at α=10° with both steady 241kPa and pulsed 172kPa AJVG blowing. The maximum hysteresis between the upstroke and downstroke C_N magnitude at a given angle of attack is $\Delta C_N \approx 0.5$ with no AJVG blowing, $\Delta C_N \approx 0.3$ with 241kPa steady blowing and $\Delta C_N \approx 0.2$ with 172kPa, 71Hz pulsed blowing. A higher average normal force can therefore be

sustained on the downstroke with the application of AJVG blowing. In addition, pulsed blowing at 71Hz can be seen to provide improved post stall C_N capability with much less mass flow requirement than steady blowing at the higher plenum pressure. A similar situation is found with $\bar{\alpha}$=14° Here the downstroke recovery occurs again at α=7° for the unblown model, but at α=9° with steady 241kPa and pulsed 172kPa AJVG blowing. The maximum hysteresis between the upstroke and downstroke C_N magnitude at a given angle of attack is $\Delta C_N \approx 0.8$ with no AJVG blowing, $\Delta C_N \approx 0.6$ with 241kPa steady blowing and $\Delta C_N \approx 0.3$ with 172kPa, 71Hz pulsed blowing.

For $\bar{\alpha}$ >14° much less benefit is seen with the application of either the steady or the pulsed AJVG blowing, with downstroke recovery occurring at about the same location in the motion for all three cases, and the hysteresis loops being, within the accuracy of the experimental instrumentation and pressure integration procedure, broadly equivalent. With $\bar{\alpha}$=16° both steady and pulsed blowing appears to prevent the large depression in C_N that occurs with no AJVG blowing between α=22 – 10° on the downstroke. In addition pulsed blowing appears to be able to suppress the sharp rise in C_N, and the corresponding peak, associated with the high level of suction on the upper surface near the leading edge due to the formation of a dynamic stall vortex, approaching maximum α on the upstroke. These peaks which are seen to occur, for both the clean model and with steady 241kPa AJVG blowing, for $\bar{\alpha}$=18° and 20°, are not present in the corresponding C_N curves with 172kPa, 71Hz, pulsed blowing.

The corresponding comparison for pitching moment coefficient is plotted on the right hand side of figure 6. It is noted that a small degree ($\Delta C_M \sim 0.02$) of hysteresis is observed, between the pitching moment on the upstroke and downstroke, even for the lowest, $\bar{\alpha}$=6°

mean angle of attack. The level of hysteresis between upstroke and downstroke pitching moment during the attached flow periods of the oscillation is practically constant for all the mean α cases, and is probably due to the inability, at the ω =12.38rad/s (k = 0.103) pitching speed, for the freestream flow on the downstroke to completely return to unstalled conditions. It was noticed that this phenomenon did not appear in the C_M data for low oscillation frequencies. For $\bar{\alpha}$=12^o both steady and pulsed air jet blowing are seen to have completely suppressed moment stall, and the subsequent period of relatively large negative (nose down) pitching moments attributed to the passage of the dynamic stall vortex as seen in the unblown model data. For the higher $\bar{\alpha}$=14^o case, the large spike in negative C_M seen in the curve with no AJVG blowing is supressed by the action of steady 241kPa blowing, but a region of high negative C_M on the early downstroke is no longer suppressed. The maximum negative C_M of -0.15 is seen to be reduced to C_M =-0.1 with pulsed AJVG blowing. For $\bar{\alpha}$>14^o there is much less of a beneficial effect of AJVG blowing on the high levels of nose down pitching moment associated with the formation, convection and shedding of the dynamic stall vortex.

One further beneficial effect of pulsed air jet blowing, indicated in the data, may be that it is capable of suppressing the period of nose up pitching moment that occurs with both steady air jet blowing and also with no blowing, in the middle of the downstroke motion. This momentary nose-up pitching moment is associated with the recovery of strong leading edge suction when much of the upper surface boundary layer still remains separated. While the levels of the nose-up pitching moment are only small, the suppression of this event will, at least, help reduce the associated fatigue on the rotor hub assembly.

4.2 The Effect of Aerofoil Pitching Rate, ω

The effect of aerofoil model pitching frequency is analysed in figure 7 where surface pressure data for sinusoidal, $\bar{\alpha}$ = 16°, $\hat{\alpha}$ = 8° pitching at ω = 1.21rad/s and 18.1rad/s are presented. First for the case of the lowest model pitching frequency of 1.21rad/s (k = 0.010), with no air jet blowing the leading edge suction peaks at about C_p =-7 at α~18° followed by a plateau until about α~20° when recovery occurs.

Full stall, with a complete loss of leading edge suction does not occur. A weak pressure ridge is evident on the rearward pressure distribution soon after primary stall. This occurs in the vicinity where a smooth drop in C_p associated with trailing edge separation is expected, the ridge may be indicative of a weak dynamic stall vortex, but there is no evidence of any strong dynamic stall vortex. With steady 241kPa (C_μ = 0.0026, F^+=1.04) AJVG blowing the leading edge suction peaks at about C_p =-9 at α~20° and is followed by a weak recovery at α~23°. Pulsed AJVG blowing (C_μ = 0.00075) results in a further increase in peak leading edge C_p to about -10 at α~22°. An earlier (α~20°) and stronger recovery occurred on the downstroke with pulsed AJVG blowing. No ridge in C_p towards the trailing edge is visible in either pressure carpet for AJVG blowing.

For the highest model pitching frequency of 18.1rad/s (k = 0.151) a strong dynamic stall vortex suction ridge is seen in the instantaneous pressure carpet with no blowing, forming at about α~23° on the upstroke and being shed at the trailing edge at ~22° on the downstroke. A similar feature is observed in the carpet for the steady 241kPa blowing case, but this is less sharp / more diffuse, indicating a weaker stall vortex. No trace of a secondary

stall vortex is evident in either pressure carpet, and in both cases the post stall leading edge C_p characteristics are practically identical, with very little suction present. With pulsed AJVG blowing the loss of leading edge suction during the stall event is not quite as abrupt as seen in the steady blowing, and inactive jet cases, and the dynamic stall vortex suction ridge is very weak indeed. Clearly pulsed AJVG blowing at the lower blowing pressure delivers a better improvement in the overall aerodynamic characteristics at this higher model pitching frequency of 18.1rad/s.

The integrated force and moment data, not presented here, suggests that the speed of the oscillatory pitching moment does not significantly affect the capability of pulsed air jet blowing to provide enhanced aerodynamic characteristics on the downstroke, whereas it can be said that as the model pitching frequency is increased, steady air jet blowing becomes less effective in enhancing the downstroke characteristics. Both steady and pulsed air jet blowing appears to be more effective on improving C_{Nmax} at the lower model pitching frequencies, the improvements becoming less the higher the pitching frequency.

4.3 The Effect of Air Jet Blowing Momentum Coefficient, C_μ

The effect of blowing pressure / blowing momentum with steady and pulsed (f=71Hz, F^+=1.04) air jet blowing is compared for ω=12.38rad/s (k = 0.103), sinusoidal, $\bar{\alpha}$ = 16°, $\hat{\alpha}$= 8° pitching, in figures 8 and 9. The instantaneous upper surface pressure carpets are presented and compared in figure 8. With no air jet blowing at all, a strong dynamic stall event is clearly evident in the surface pressure response, with a strong primary dynamic stall vortex suction ridge followed by a weaker secondary suction ridge. The effect of steady AJVG blowing at 241kPa (C_μ = 0.0026) is seen to be the near, if not complete,

suppression of the secondary stall vortex and the prevention of the complete loss of leading edge suction on the downstroke – a secondary suction peak being clearly evident. 71Hz pulsed blowing at 241kPa (C_μ = 0.0013) was found to provide a similar result but with a weaker, more dissipated, primary stall vortex suction ridge, and no evidence of any secondary suction ridge at all.

With steady blowing at 328kPa (C_μ = 0.0046) a primary stall vortex suction ridge is still evident, though it is seen to be very weak, but with 71Hz pulsing at 310kPa (C_μ = 0.00205, F^+=1.04) there does not appear to be any evidence at all of any stall event. The leading edge suction undergoes the sinusoidal variation expected of a near inviscid flow, and no suction stall vortex ridge is seen at all. This is a remarkable result since this almost complete stall suppression is achieved with less than half of the total mass flow rate of the steady 328kPa blowing case. This sinusoidal pitching case with $\bar{\alpha}$ = 16°, $\hat{\alpha}$ = 8°, is a relatively severe case with a maximum angle of attack of 24°, but pulsed AJVG blowing has been shown capable of practically suppressing dynamic stall.

In figure 9 the curves of the behaviour of C_N and C_M during the pitch cycle are presented for both steady and pulsed blowing at different blowing momentum coefficients. For the steady air jet blowing cases, a blowing pressure of 145kPa (C_μ = 0.0011) is seen to significantly reduce but not completely suppress the occurrence of the C_N peak due to the contribution of the dynamic stall vortex suction at the end of the upstroke. With no air jet blowing, the nonlinear rise in C_N due to the formation of the stall vortex is seen to begin at α=23° on the upstroke. With 145kPa steady air jet blowing, this is delayed until just prior to the beginning of the downstroke at α=24°. Steady blowing at an increased 248kPa (C_μ = 0.0028) achieves the same result, but a further increase in blowing pressure to 328kPa

(C_μ = 0.0046) is seen to completely suppress this C_N peak suggesting that in this case the dynamic stall vortex is significantly weakened, or even completely suppressed. Steady 145kPa blowing was also found to increase the C_N level on the latter period of the downstroke (α =18-10^o) compared with that obtained with inactive air jets. In the early period of the downstroke, however, the C_N levels were found to be slightly below those calculated for the inactive air jet case. The small recovery in C_N observed in the inactive air jet case for α =23-22^o, which is possibly associated with the formation of a secondary stall vortex which creates suction lift as it proceeds downstream over the upper surface, is also seen with 145kPa steady blowing, but beginning at a lower C_N level. With 248kPa steady air jet blowing this C_N recovery begins later at some 2^o angle of attack further into the downstroke before the C_N curve plateaus out at a level ~10% higher than that seen with the lower blowing pressure. With 328kPa blowing pressure the primary stall event, which now takes place on the commencement of the downstroke movement, becomes much more benign, with no abrupt loss of normal force but a gradual reduction followed by a plateau at the same level as that seen with 248kPa blowing pressure.

Clearly an increase in steady blowing pressure, and thereby the blowing momentum coefficient, results in a beneficial improvement in the C_N characteristics, especially on the downstroke, where up to 40% increased normal force can be sustained over and above the levels maintained without air jet blowing. The corresponding result for pulsed AJVG blowing at a constant 71Hz (F^+ = 1.04) pulsing frequency, 50% duty cycle condition, is presented in figure 9b). Here a very similar result is found, but the sensitivity with blowing pressure is seen to be much enhanced. A comparison between the C_N curves for steady blowing at 328kPa, and pulsed blowing at the lower 310kPa, shows that pulsing at 71Hz,

with a mass flow rate of just less than half, results in significantly improved C_N levels on the downstroke – with levels up to twice those seen with no air jet blowing. From this it is clear that a further significant improvement in C_N characteristics is achieved with pulsed blowing, with at least a halving of the mass flow requirement, and that this benefit is seen to be greater the higher the average blowing pressure and associated value of C_μ.

The corresponding plots of the pitching moment characteristics reveal that steady blowing is seen to promote a later, but more severe moment stall. However, a blowing pressure of 248kPa is seen to have slightly reduced the maximum pitch down moment, while an increase to 328kPa results in a further dramatic reduction, with a peak negative pitching moment coefficient of 40% of that seen without any air jet blowing. In addition steady air jet blowing, at all blowing pressures investigated, was seen to promote an earlier recovery on the downstroke, compared with the clean aerofoil case. Also, while the period during which a small positive (nose up) pitching moment is experienced on the latter stages of the downstroke is extended with steady air jet blowing, it is seen that with the highest 328kPa blowing pressure, the maximum level has been suppressed. With pulsed blowing, a blowing pressure of 172kPa is seen to have significantly reduced the peak nose down pitching moment on the commencement of the downstroke, compared with no effect with 97kPa steady blowing. Further increases in blowing pressure are seen to have further reduced this peak negative pitching moment coefficient until, with 310kPa there does not appear to be any significant trace of a strong moment stall at the onset of the downstroke, and through a large extent of the downstroke the C_M level is reduced to nearly zero. The pitching moment data therefore also shows that worthwhile aerodynamic benefits can be

achieved by pulsing the air jets as long as the blowing pressure is not too low (in this case below about 138kPa).

4.4 The Effect of Air Jet Pulsing Frequency, *f*

The effect of pulsing frequency is analysed in figure 10 for this same $\bar{\alpha}$ =16º, $\hat{\alpha}$=±8º case with a nominal plenum pressure of 172kPa giving C_μ = 0.0015, or an effective C_μ of 0.00075 for a pulsed jet duty cycle of 50%. For this case the instantaneous upper surface pressure carpets, showed that 20Hz, F^+=0.29, pulsing was not effective in suppressing even the secondary stall vortex suction ridge. Increasing the pulsing frequency to 50Hz, F^+=0.73, resulted in the effective suppression of the secondary suction ridge, while the primary suction ridge was marginally weakened. Further increasing the pulsing frequency was found not to further improve the upper surface pressure response, the primary suction ridge still being clearly evident with the highest pulsing frequency of 200Hz, F^+=2.93.

Close inspection of the normal force curves, presented in figure 10, shows that pulsed AJVGs are effective in suppressing the non-linear "spike" in normal force at the top of the upstroke due to the suction of the forming dynamic stall vortex. With no air jet blowing, and with steady AJVG blowing a secondary suction peak is seen to occur in the early stages of the downstroke, due to a secondary stall vortex formation. This feature is also seen, but at a later stage in the downstroke, in the curve for pulsed blowing at 20Hz (F^+=0.29), but with higher pulsing frequencies this secondary feature is suppressed.

Inspection of the all the curves for C_N, and C_M shows that there is a big difference between the results achieved with 20Hz pulsing and with 50Hz, F^+=0.73, and higher. With 50Hz, F^+=0.73, pulsing or above, the aerodynamic improvements are at least as good, if

not considerably better than the equivalent steady blowing, while 20Hz is not as effective. This is in good agreement with the finding of an earlier study on this model (Ref. 23) which showed that, for quasi-static pitching, pulsed jets need to be run at 35Hz or higher (corresponding with the measured trailing edge natural shedding frequency) to achieve their full aerodynamic effectiveness. From the results presented in figure 11, it is not clear which pulsing frequency – 50Hz or above, is most effective in maximising C_N, for a given angle of attack, while limiting the level of C_M divergence. Pulsing in the frequency range 50Hz-140Hz, (F^+=0.73 – 2.05) appears to achieve very similar results, while the results for the highest 200Hz, F^+=2.93 pulsing on the later period of the downstroke do not appear to be quite as good. With the limited results obtained, pulsing in the range F^+=0.5 – 1.00 therefore seems to be the most optimum setting for enhanced aerodynamic performance with 172kPa blowing pressure (C_μ = 0.00075).

4.5 The Effect of Air Jet Duty Cycle, *DC*

The effect of pulsed jet duty cycle, *DC*, (the percentage of time during a pulse cycle, during which the jet is active) was investigated for the $\bar{\alpha}$ =16^o and $\hat{\alpha}$=±8^o case with a nominal 172kPa plenum pressure (C_μ = 0.0015) and constant 71Hz pulsing frequency (F^+ = 1.04). Close inspection of the computed C_N and C_M characteristics showed that, for the different duty cycle cases investigated, there was no obvious benefit in pulsing with duty cycle higher than the 50%. Interestingly there was no large degradation in performance in operating the pulsed air jets with duty cycle settings as low as 25%.

These results suggest that there is some benefit in reducing the duty cycle from 50% to somewhere in the region of 30-40%, since the overall mass flow requirement can be

significantly reduced without significantly impacting on the aerodynamic performance enhancements.

4.6 Overall Comparisons

To properly compare the relative benefits of pulsed air jet blowing versus purely steady blowing, figure 11 plots, for the case of a constant cyclic pitch of 8°, the variations with collective pitch, $\bar{\alpha}$, of the maximum normal force achieved during the cycle, the corresponding minimum pitching moment and the damping coefficient for the unblown and for steady (C_μ = 0.0026) and pulsed blowing (C_μ = 0.00075) cases. The damping coefficient, a, is defined as:

$$a = \frac{-C_w}{\pi \hat{\alpha}^2}$$

where C_w is the work coefficient, given by:

$$C_w = \oint C_M(\alpha) d\alpha$$

where angles are expressed in radians, and is a measure of the work done per cycle by the pitching moment. Air jet blowing should, ideally, reduce the maximum normal force caused by the stall vortex suction peak, and the corresponding minimum pitching moment which are both responsible for excessive fatigue loading of the blade and its hub.

Up to 10° collective pitch the action of air jet blowing does not affect the maximum normal force or the minimum pitching moment. At $\bar{\alpha} = 12°$ the jump in minimum pitching moment that occurs in the baseline case is suppressed by both steady and pulsed air jet blowing. At 14° collective pitch and higher, the pulsed blowing is seen to significantly reduce (by up to 10%) the maximum normal force below that experienced by the baseline model, while

steady blowing at over three times C_μ , can only match this performance at $\bar{\alpha} = 14^o$ and cannot provide any improvement at the highest collective pitch angles. At these angles this much weaker air jet pulsing is also seen to be able to better reduce the minimum pitching moment compared with the more powerful steady blowing.

Positive cycle damping is desirable, and while a clockwise portion of a C_M~α cycle is negatively damped a positive net cycle damping is possible. Negative damping is potentially adverse, however, as it may lead to stall flutter, and is known to be a consequence of a deep dynamic stall (Ref 31). The damping coefficient usefully summarises the net effect within a C_M~α cycle in a particularly meaningful way. All the cases show positive damping at the lowest mean angle of $\bar{\alpha} = 14^o$. The unblown case shows negative damping at all the higher mean angles. Steady blowing delays the onset of negative damping to just beyond $\bar{\alpha} = 14^o$, and pulsed blowing shows low but still positive damping at $\bar{\alpha} = 14^o$. In each case this is associated with the attenuation of the dynamic stall due to the blowing.

This study further confirms the findings of others, that pulsed air jet vortex generators offer significant performance improvement over purely steady blowing. This work demonstrates that this can be achieved with considerably reduced values of C_μ, and corresponding mass flow. Since these effects are known to be achieved by the enhanced mixing within the boundary layer, and not by any disturbance of the external outer flow which would, in fact be detrimental. This is why very low momentum blowing designed to maximize the production of vorticity deep within the boundary layer can be very effective.

Conclusions

The present experiments on a sinusoidal pitching RAE9645 aerofoil section model have demonstrated that steady air jet blowing tended to increase C_{Nmax}, reduce peak negative pitching moment and delay the occurrence of primary and full stall to a higher angle of attack as well as incipient drag rise. Increasing the blowing pressure, and thereby the jet to freestream velocity ratio, was found to accentuate these beneficial effects. Pulsed air jet blowing in the pulsing frequency range $F^+ = 0.5 – 1.0$ was found to further increase C_{Nmax} and further delayed the occurrence of primary and full stall over and above that achieved with corresponding steady air jet blowing. An effective duty cycle range of 0.4 - 0.75 was recorded. This means that similar aerodynamic improvements as obtained with steady air jet blowing can be achieved with pulsed blowing but with considerably reduced air mass flow rate requirements. For moderate mean angles of attack cases where dynamic stall occurred at the higher angles of attack of the cycle, steady blowing was found capable of suppressing the formation of the dynamic stall vortex, preventing the occurrence of the non-linear rise in C_N linked with dynamic stall vortex suction. Pulsed AJVGs were found to be even more effective, achieving the improved performance with considerably reduced air mass flow requirement, and were found capable of reducing, and even suppressing, the vortex suction ridge in the instantaneous upper surface C_p carpets, over and above the capability of steady air jet blowing at the same blowing pressure. Pulsed blowing was also found to be more effective in maintaining residual levels of leading edge suction, and therefore the C_N levels, during the downstroke. Pulsed air jet blowing was found to be optimum in the range $F^+ = 0.5 – 1.0$ with DC=0.4 - 0.5.

Acknowledgments

This work was funded under the UK Defence Applied Research Partnership program, by the UK Defence Science & Technology Laboratory, QinetiQ Ltd., AgustaWestland Ltd. and the Technology Strategy Board.

References

[1]McAlister, K. W., Carr, L. W. and McCroskey, W. J, "Dynamic Stall Experiments on the NACA 0012 Airfoil", NASA TP 1100. 1978.

[2]Carr, L. W., "Progress in the Analysis and Prediction of Dynamic Stall" *Journal of Aircraft*, Vol. 25, No. 1, 1988, pp 6 – 17.

[3]Wallis, R. A., "The Use of Air Jets for Boundary Layer Control," Aeronautical Research Labs, Aero. Note 110, Melbourne, Australia, 1952.

[4]Freestone, M., "Preliminary Tests at Low Speeds on the Vorticity Produced by Air-Jet Vortex Generators," City University, Department of Aeronautics Research Memo. 85/1, London, Feb. 1985.

[5]Pauley, W. R., and Eaton, J. K., "Experimental Study of the Development of Longitudinal Vortex Pairs Embedded in a Turbulent Boundary Layer," *AIAA Journal*, Vol. 26, No. 7, 1988, pp. 816–823. doi:10.2514/3.9974

[6]Johnston, J. P., and Nishi, M., "Vortex Generator Jets: A Means of Flow Separation Control," *AIAA Paper* 1989-0564, 1989.

[7]Selby, G. V., Lin, J. C., and Howard, F. G., "Control of Low-Speed Turbulent Separated Flow Using Jet Vortex Generators," *Experiments in Fluids*, Vol. 12, No. 6, 1992, pp. 394–400. doi:10.1007/BF00193886

[8]Compton, D. A., and Johnston, P., "Streamwise Vortex Production by Pitched and Skewed Jets in a Turbulent Boundary Layer," *AIAA Journal*, Vol. 30, No. 3, 1992, pp. 640–647. doi:10.2514/3.10967

[9]Henry, F. S., and Pearcey, H. H., "Numerical Model of Boundary Layer Control Using Air-Jet Generated Vortices," *AIAA Journal*, Vol. 32, No. 12, 1994, pp. 2415–2424. doi:10.2514/3.12308

[10]Zhang, X., and Collins, M. W., "Nearfield Evolution of a Longitudinal Vortex Generated By Inclined Jet in a Turbulent Boundary Layer," *Journal of Fluids Engineering*, Vol. 119, No. 4, Dec. 1997, pp. 934–939. doi:10.1115/1.2819520

[11]Oyler, T. E., and Palmer, W. E., "Exploratory Investigation of Pulsed Blowing for Boundary Layer Control," North American Rockwell Corp. Rept. NR 72H-12, 1972.

[12]Seifert, A., Bachar, T., Koss, D., Shepshelovich, M., and Wygnanski, I., "Oscillatory Blowing: A Tool to Delay Boundary Layer Separation" *AIAA Journal*, Vol. 31, No. 11, 1993, pp. 2052–2060. doi:10.2514/3.49121.

[13]McManus, K. R., Ducharme, A., Goldley, C., and Magill, J., "Pulsed Jet Actuators for Suppressing Flow Separation," 34th AIAA Aerospace Sciences Meeting and Exhibit, Reno, NV, AIAA Paper 1996-0442, Jan. 1996.

[14]McManus, K. R., Legner, H. H., and Davis, S. J., "Pulsed Vortex Generator Jets for Active Control of Flow Separation," 25th AIAA Fluid Dynamics Conference, Colorado Springs, CO, AIAA Paper 19942218, June 1994.

[15]Seifert, A., Darabi, A., and Wygnanski, I., "Delay of Airfoil Stall by Periodic Excitation" *Journal of Aircraft*, Vol. 33, No. 4, 1996, pp. 691–698. doi:10.2514/3.47003

[16]McManus, K. R., Joshi, P. B., Legner, H. H., and Davis, S. J., "Active Control of Aerodynamic Stall Using Pulsed Jet Actuators," 26th AIAA Fluid Dynamics Conference, AIAA Paper 1995-2187, June 1995.

[17]McManus, K. R., Ducharme, A., Goldey, C., and Magill, J., "Pulsed Jet Actuators for Suppressing Flow Separation," 34th Aerospace Sciences Meeting and Exhibit, Reno NV, AIAA Paper 1996-0442, Jan. 1996.

[18]McManus, K. R., and Magill, J., "Separation Control in Incompressible and Compressible Flow Using Pulsed Jets," AIAA Paper 1996-1948, June 1996.

[19]Magill, J. C., and McManus, K. R., "Control of Dynamic Stall Using Pulsed Vortex Generator Jets," 36th Aerospace Sciences Meeting and Exhibit, Reno, NV, AIAA Paper 1998-0675, 1998.

[20]Greenblatt, D., "Dual Location Separation Control on a Semispan Wing," *AIAA Journal*, Vol. 45, No. 8, 2007, pp. 1848–1860. doi:10.2514/1.27757.

[21]Scholz, P., Casper, M., Ortmanns, J., Kähler, C., and Radespiel, R., "Leading-Edge Separation Control by Means of Pulsed Vortex Generator Jets," *AIAA Journal*, Vol. 46, No. 4, April 2008, pp. 837–846. doi:10.2514/1.26176

[22]Ortmanns, J., Bitter, M., and Kahler, C. J., "Dynamic Vortex Structures for Flow-Control Applications" *Experiments in Fluids*, Vol. 44, No. 3, 2008, pp. 397–408. doi:10.1007/s00348-007-0442-8

[23]Prince, S. A. & Khodagolian, V, "Low-Speed Static Stall Suppression Using Steady and Pulsed Air-Jet Vortex Generators", *AIAA Journal*, Vol. 49, No. 3, 2011, pp642-654. doi: 10.2514/1.J050754

[24]Greenblatt, D., and Wygnanski, I., "Dynamic Stall Control by Oscillatory Addition of Momentum. Part 1: NACA 0015 Parametric Study," *Journal of Aircraft*, Vol. 38, No. 3, 2001, pp. 430–438. doi:10.2514/2.2810

[25]Greenblatt, D., Nishri, B., Darabi, A., and Wygnanski, I., "Dynamic Stall Control by Oscillatory Addition of Momentum. Part 2: Mechanisms," *Journal of Aircraft*, Vol. 38, No. 3, 2001, pp. 439–447. doi:10.2514/2.2811

[26]Weaver, D., McAlister, K. W. and Tso, J. "Control of vr-7 dynamic stall by strong steady blowing". *Journal of Aircraft*, 41(6):1404-1413, 2004. Doi:10.2514/1.4413

[27]Gardner, A.D., Richter, K., Mai, H., and Neuhaus, D. "Experimental investigation of high-pressure pulsed blowing for dynamic stall control". *CEAS Aeronautical Journal*, 5:185-198, 2014. doi:10.1007/s13272-014-0099-y

[28]Müller-Vahl, H. F., Nayeri, C. N., Paschereit, C. O., and Greenblatt, D. "Dynamic stall control via adaptive blowing". *Renewable Energy*, 97:47-64, 2016. doi:10.1016/j.renene.2016.05.053.

[29]Singh C, Peake D J, Kokkalis A, Coton F and Galbraith R, "Control of flow on helicopter rotor blades under quasi-steady and unsteady flow conditions using smart air-jet vortex generators", Proc of 29th European Rotorcraft Forum, Germany, 16-18 September 2003.

[30]Singh, C, Peake D J, Coton F, Kokkalis A, and Galbraith R A, "The application of air-jet vortex generators to suppress flow separation on helicopter rotor aerofoil sections under quasi-steady and unsteady conditions", AIAA Paper 2004-0045.

[31]Carta, F. O., "An Analysis of the Stall Flutter Instability of Helicopter Rotor Blades," Journal of the American Helicopter Society, Vol. 12, No. 4, 1967, pp. 1–18. doi:10.4050/JAHS.12.1

List of Figures

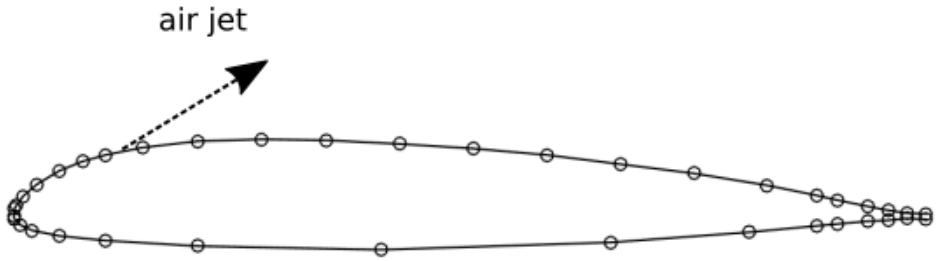

Fig. 1. Chordwise profile of the RAE9645 aerofoil section with AJVG array and pressure transducer locations (indicated by symbols).

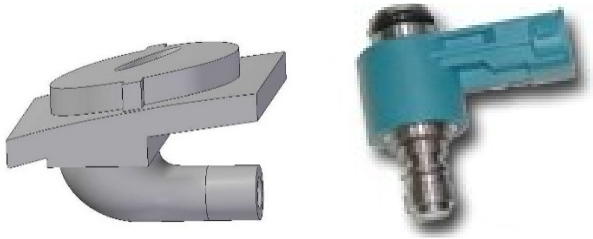

a) AJVG nozzle insert b) The Synerject air injector

Fig. 2. Details of the air injector implementation.

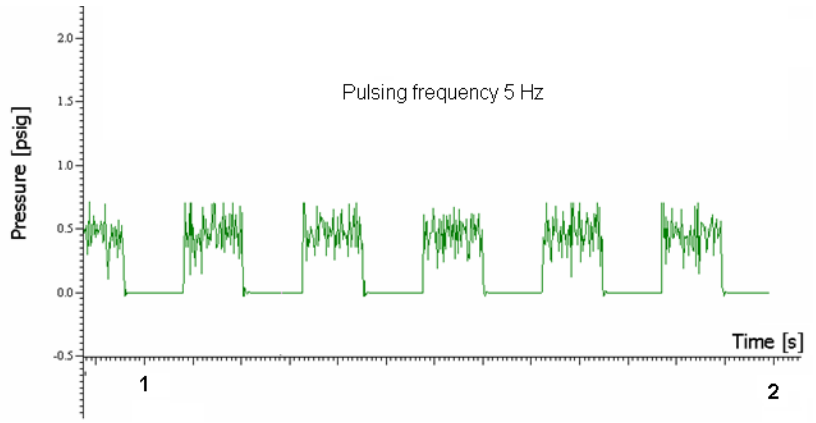

Fig. 3. Example of the fluctuating jet exit pressure versus time, for a square wave input pulsing wave form with zero freestream velocity.

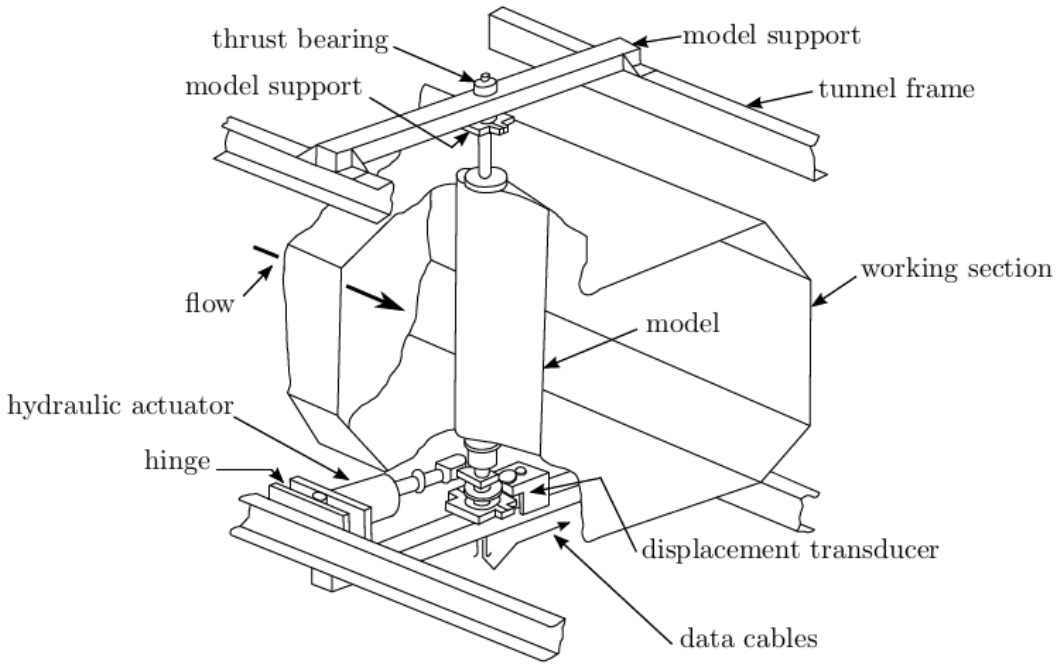

Fig. 4. Schematic of the Glasgow University Dynamic Stall Rig.

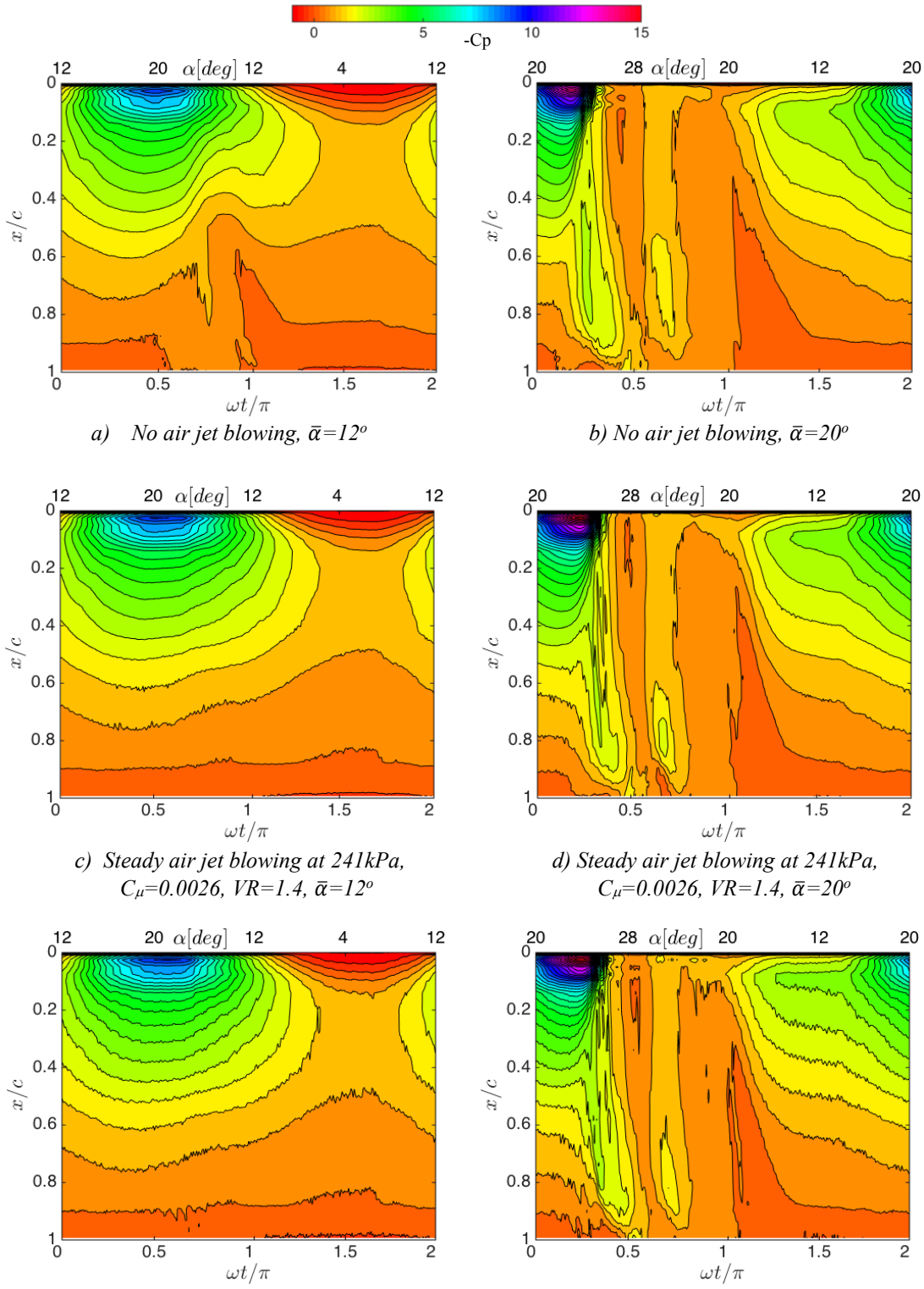

a) No air jet blowing, $\bar{\alpha}$=12°

b) No air jet blowing, $\bar{\alpha}$=20°

c) Steady air jet blowing at 241kPa, C_μ=0.0026, VR=1.4, $\bar{\alpha}$=12°

d) Steady air jet blowing at 241kPa, C_μ=0.0026, VR=1.4, $\bar{\alpha}$=20°

e) Pulsed air jet blowing at 172kPa, C_μ=0.00075, VR=1.2, $\bar{\alpha}$=12°, f=71Hz, F^+= 1.04, DC=0.5

f) Pulsed air jet blowing at 172kPa, C_μ=0.00075, VR=1.2, $\bar{\alpha}$=20°, f=71Hz, F^+= 1.04, DC=0.5

Fig. 5. *Comparison between upper surface pressure distribution versus α for mean pitch angles of 12° and 20° with and without air jet blowing, $\hat{\alpha}$=±8°, ω=12.38rad/s, k=0.103 pitching, U_∞=30m/s, Re_c=1.0x10^6.*

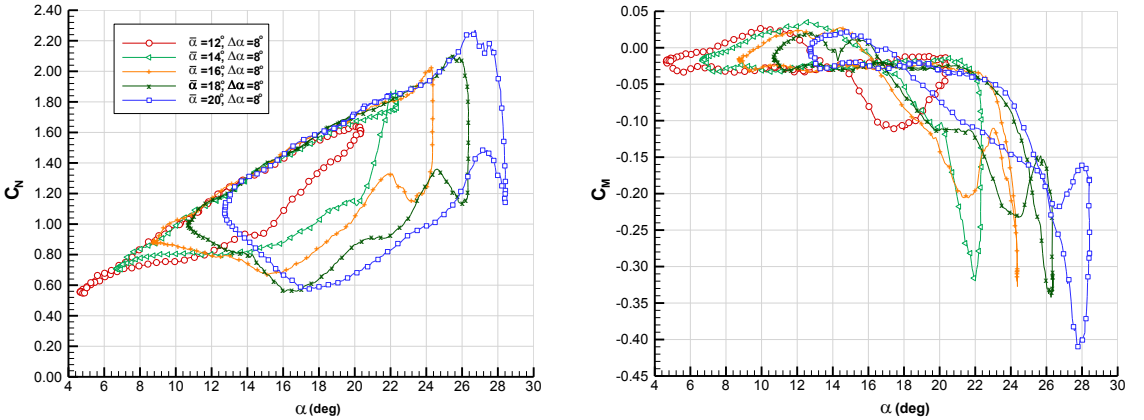

a) No air jet blowing

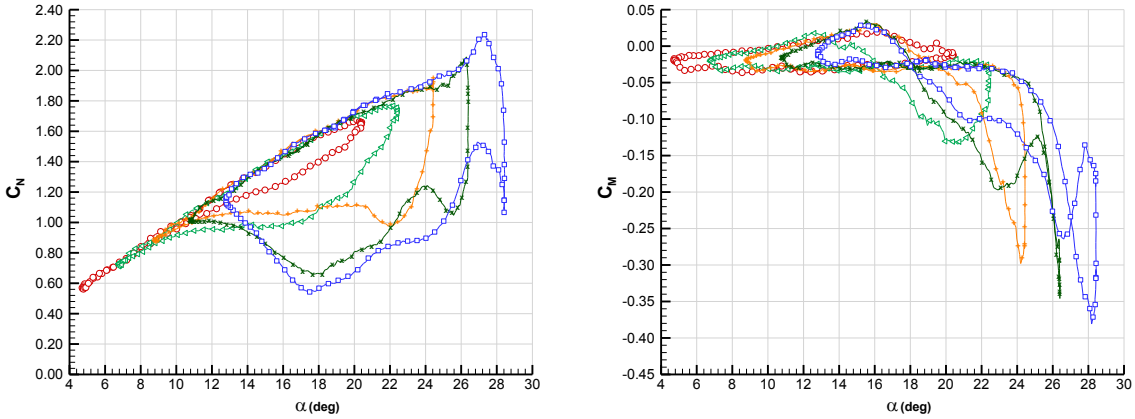

b) Steady air jet blowing at 241kPa, C_μ=0.0026, VR = 1.4

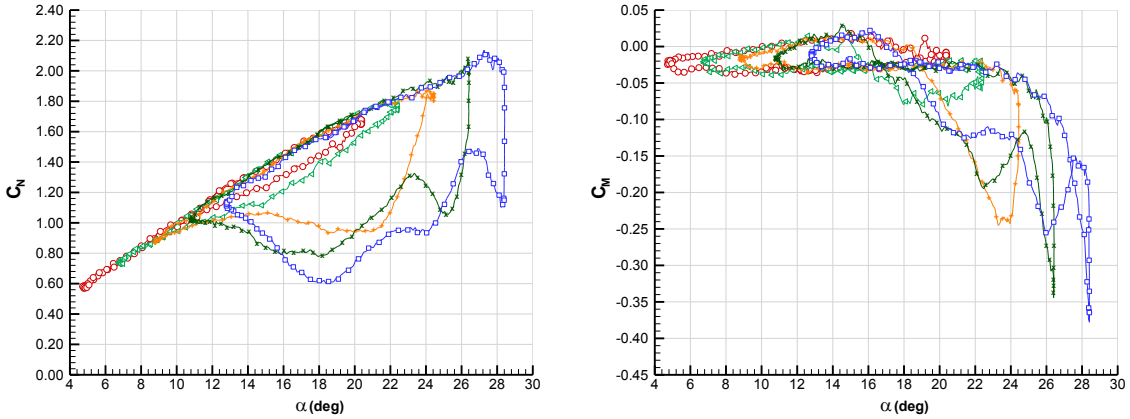

c) Pulsed air jet blowing at 172kPa, C_μ=0.00075, VR=1.2, f=71Hz, F^+=1.04, DC=0.5

Fig. 6. *C_N and C_M characteristics for $\hat{\alpha}=\pm 8^o$, ω=12.38rad/s (k=0.103) sinusoidal pitching, with varying mean pitch angle. U_∞=30m/s, Re_c=1.0x10^6*

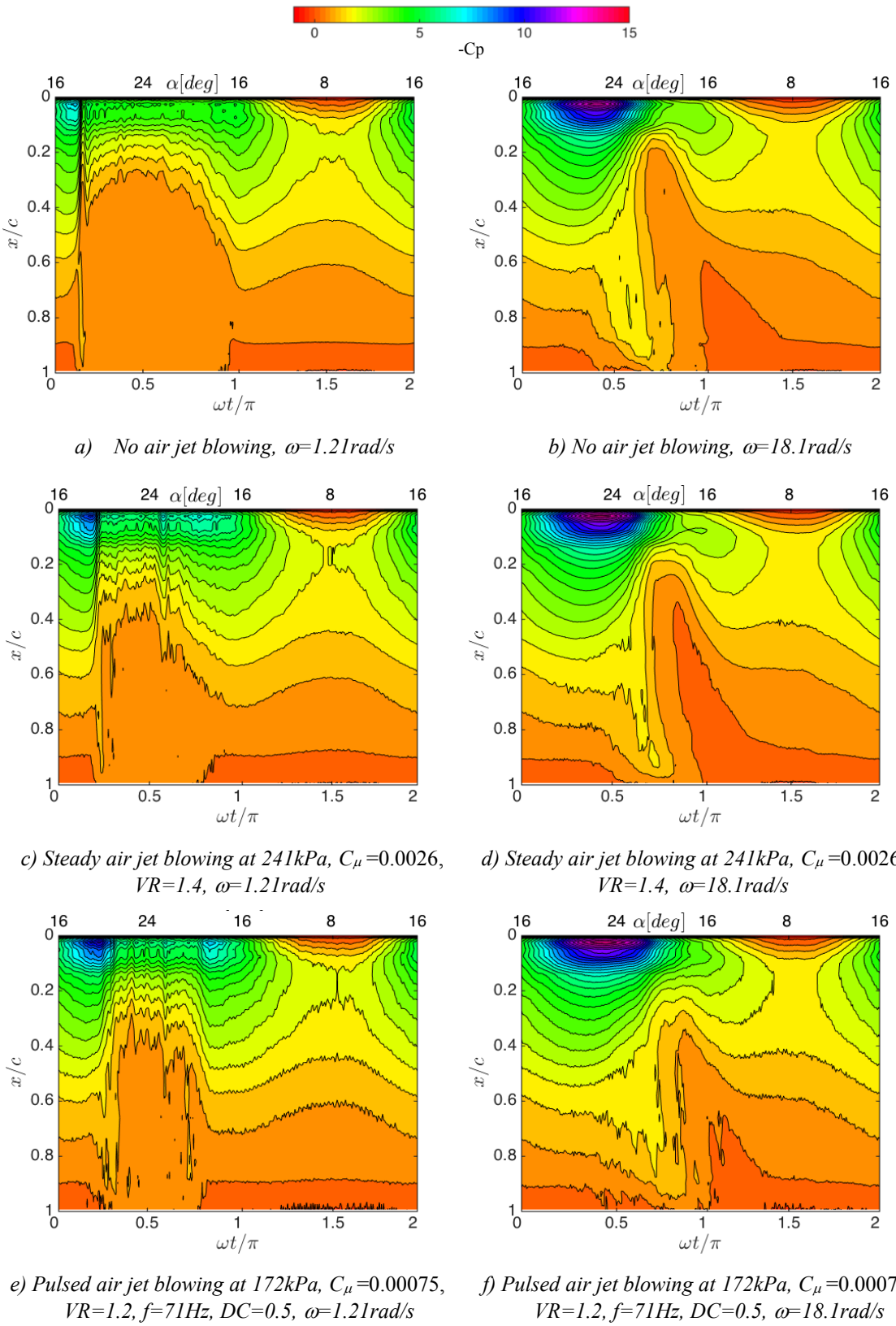

a) No air jet blowing, ω=1.21rad/s

b) No air jet blowing, ω=18.1rad/s

c) Steady air jet blowing at 241kPa, C_μ=0.0026, VR=1.4, ω=1.21rad/s

d) Steady air jet blowing at 241kPa, C_μ=0.0026, VR=1.4, ω=18.1rad/s

e) Pulsed air jet blowing at 172kPa, C_μ=0.00075, VR=1.2, f=71Hz, DC=0.5, ω=1.21rad/s

f) Pulsed air jet blowing at 172kPa, C_μ=0.00075 VR=1.2, f=71Hz, DC=0.5, ω=18.1rad/s

Fig 7. *Comparison of upper surface Cp distributions, $\bar{\alpha}$=16°, $\hat{\alpha}$=±8°, pitching at frequencies of ω =1.21rad/s (k=0.01) and 18.1rad/s (k=0.151), U_∞=30m/s, Re_c=1.0x10^6*

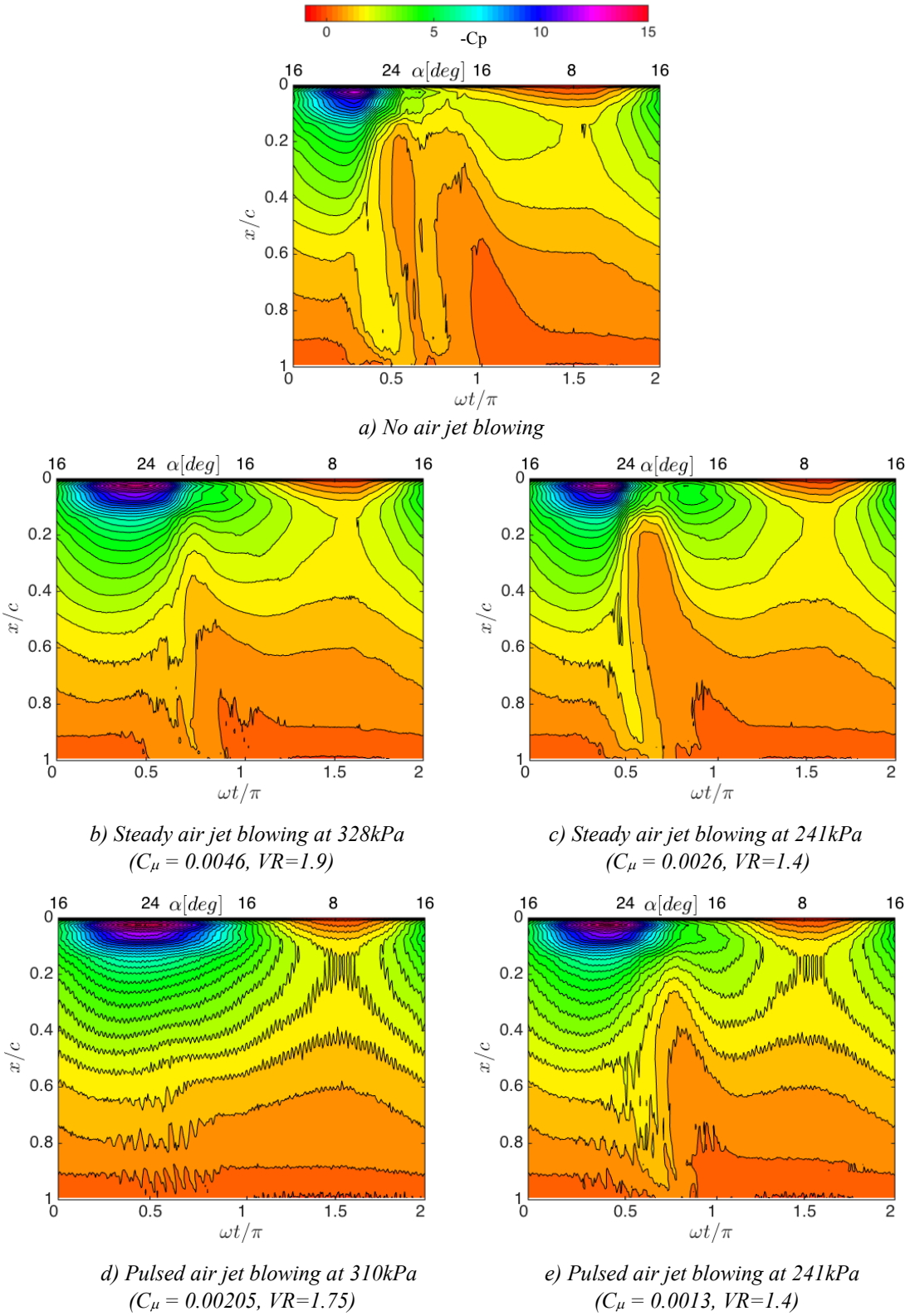

a) No air jet blowing

b) Steady air jet blowing at 328kPa (C_μ = 0.0046, VR=1.9)

c) Steady air jet blowing at 241kPa (C_μ = 0.0026, VR=1.4)

d) Pulsed air jet blowing at 310kPa (C_μ = 0.00205, VR=1.75)

e) Pulsed air jet blowing at 241kPa (C_μ = 0.0013, VR=1.4)

Fig 8. *Comparison between upper surface pressure distribution versus α for steady and pulsed (f=71Hz, F^+ =1.04) air jet blowing at ~310kPa and ~241kPa, $\bar{\alpha}$=16°, $\hat{\alpha}$=±8°, ω =12.38rad/s (k =0.103) pitching, U_∞=30m/s, Re_c=1.0x10^6*

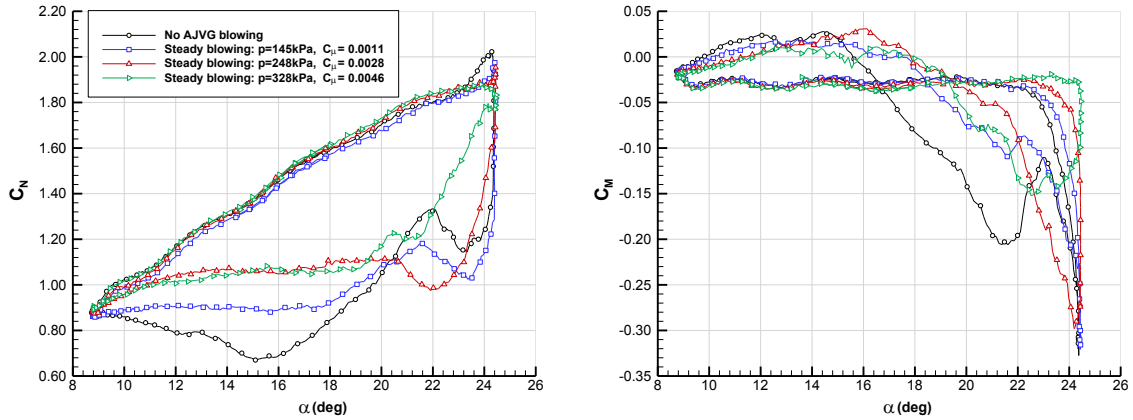

a) Steady air jet blowing

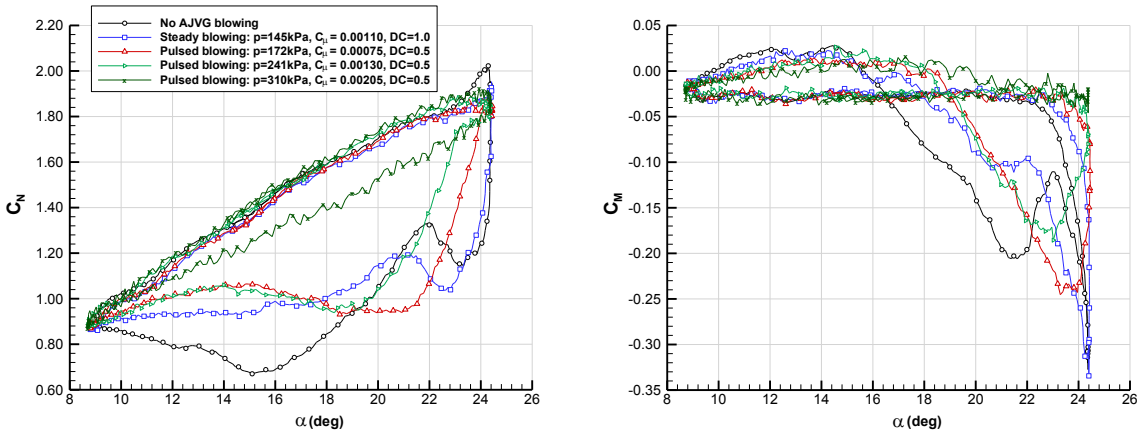

b) Pulsed air jet blowing, f=71Hz, DC=0.5

Fig. 9. *C_N and C_M characteristics for steady and pulsed air jet blowing at different blowing pressures. Sinusoidal, $\bar{\alpha}$=16°, $\hat{\alpha}$=±8°, ω=12.38rad/s (k=0.103) pitching, U_∞=30m/s, Re_c=1.0x10^6*

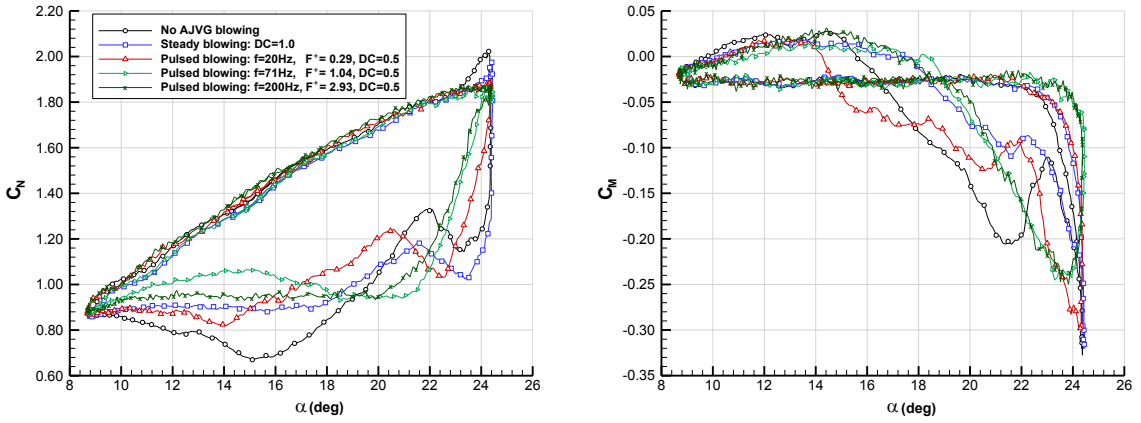

Fig. 10. *C_N and C_M characteristics for pulsed air jets with varying pulsing frequency. $\bar{\alpha}$=16°, $\hat{\alpha}$ =±8°, ω=12.38rad/s (k = 0.103) pitching, p=172kPa (C_μ = 0.0015, VR=1.2 for steady blowing), U_∞=30m/s, Re_c=1.0x10^6*

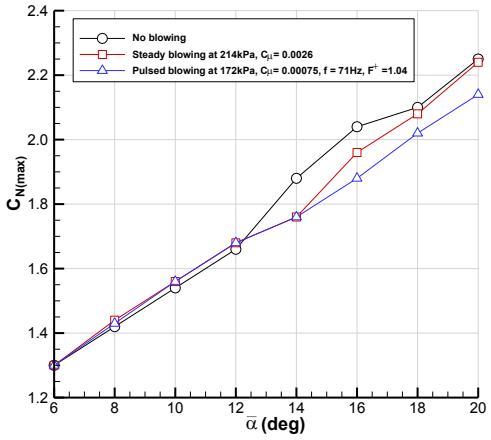

a) Maximum normal force

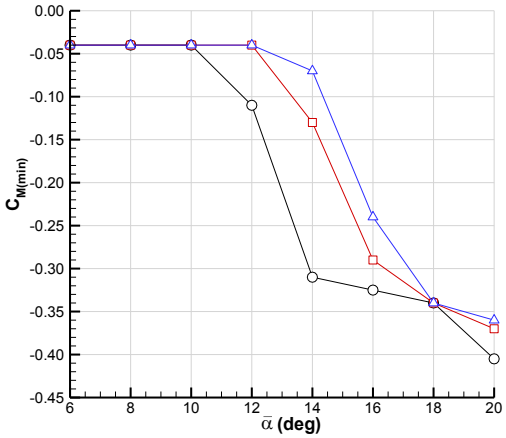

b) Minimum pitching moment

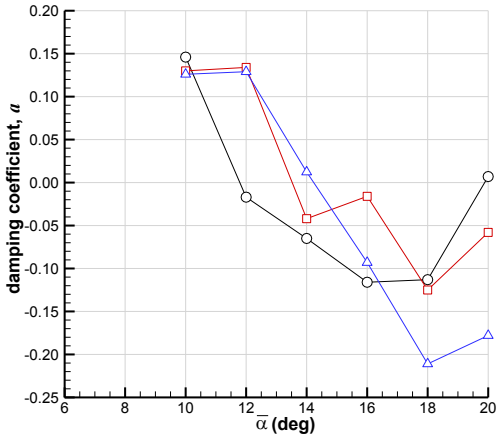

c) Damping coefficient

Fig. 11. *Variation of the maximum normal force, minimum pitching moment and the damping coefficient with collective pitch setting for $\hat{\alpha}=\pm 8^o$, $\omega=12.38$rad/s ($k = 0.103$) pitching, $U_\infty=30$m/s, $Re_c=1.0x10^6$*

2019-07-01

The effect of steady and pulsed air jet vortex generator blowing on an aerofoil section model undergoing sinusoidal pitching

Prince, Simon A.

Vertical Flight Society

Prince S, Green F, Coton F, Wang Y. (2019) The effect of steady and pulsed air jet vortex generator blowing on an aerofoil section model undergoing sinusoidal pitching. Journal of the American Helicopter Society, Volume 64, Issue 3, July 2019, pp.1-14

https://doi.org/10.4050/JAHS.64.032004